

Electronic Supplementary Information (ESI)

Effect of Nanosilver Surface on Peptide Reactivity Towards Reactive Oxygen Species

Erik Jacques¹, Manuel Ahumada^{1,6}, Brianna Rector², Goonay Yousefalizadeh²,
Constanza Galaz-Araya³, Rodrigo Recabarren³, Kevin Stampelcoskie^{2*}, Horacio
Poblete^{3,4*}, Emilio I. Alarcon^{1,5*}

¹Bio-Nanomaterials Chemistry and Engineering Laboratory, Division of Cardiac Surgery, University of Ottawa Heart Institute, 40 Ruskin Street, Ottawa, Ontario, K1Y 4W7, Canada. ²Queen's University, Chemistry, Chernoff Hall Rm 505/435 [90 Bader Lane, Kingston, Ontario, Canada, K7L 3N6](#). ³Center for Bioinformatics and Molecular Simulations, Facultad de Ingeniería, Universidad de Talca, Chile. ⁴Millennium Nucleus of Ion Channels-Associated Diseases (MiNICAD), Universidad de Talca, 3460000 Talca, Chile. ⁵Department of Biochemistry, Microbiology, and Immunology, University of Ottawa, Ottawa, Ontario, Canada. ⁶ Centro de Nanotecnología Aplicada, Facultad de Ciencias, Universidad Mayor, Chile.

*Corresponding authors

Emails: Ealarcon@ottawaheart.ca; kevin.stampelcoskie@queensu.ca; hopoblete@utalca.cl

Page S1. This page

Pages S2-S6. Materials and Methods and experimental.

Page S7. Figure S1. Plasmonic absorption for citrate capped nanosilver in the presence of AAPH at 37°C.

Page S8. Figure S2. Effect of nanosilver addition on the fluorescence emission of WP1.

Page S9. Figure S3. Effect of 10 mM NaCl media in the surface plasmon band absorption for nanosilver without peptides.

Page S10. Figure S4. Hydrodynamic size and surface charge for nanosilver without and with WP1, WP2, and WP3.

Page S11. Figure S5. Steady state absorbance spectra of Ag cluster samples stabilized by peptides.

Page S12. Figure S6. 2D fsTAS profiles for Ag clusters stabilized by P2, WP3, P3 and WP3.

Page S13. Figure S7. Transient absorption spectra for Ag clusters stabilized with P2 and WP2.

Page S14. Figure S8. Transient absorption spectra for Ag clusters stabilized with P3 and WP3.

Page S15. Figure S9. Characterization of the binding mode of WP1, WP2, and WP3 to the AgNP surface through molecular simulations.

Page S16. References.

Materials and Methods

Chemical reagents: Silver nitrate (AgNO_3), 2-hydroxy-1-[4-(2-hydroxyethoxy)phenyl]-2-methyl-1-propanone (I-2959), 2,2'-azobis(2-amidinopropane) dihydrochloride (AAPD), Trisodium 2-hydroxypropane-1,2,3-tricarboxylate (sodium citrate), sodium hydroxide (NaOH), phosphate buffered saline (PBS), dimethyl sulfoxide (DMSO) and sodium chloride (NaCl) ordered from Sigma-Aldrich were used as received. Custom synthesized peptides (purity > 95%): WP1: (CLKGP-Hyp-W, M-W = 815.98), WP2: (CLKGP-Hyp-GP-Hyp-GP-Hyp-W, M-W = 1350.73) and WP3: (CLKGP-(Hyp-GP)₄-Hyp-W, M-W = 1885.10) from abm® were used as received. Unless otherwise indicated, all solutions were prepared using Milli-Q water.

Synthesis of citrate protected nanosilver: Citrate protected nanosilver was prepared using a previously described protocol.¹ Briefly, an aqueous solution containing 0.2 mM AgNO_3 , 0.2 mM I-2959 and 1 mM sodium citrate was purged with nitrogen gas for 30 min to deoxygenate the solution. Once purged, the solution was UVA light irradiated (8 lamps) at 25°C in a temperature controlled Luzchem LZC-4 photoreactor (Ottawa, CA) for 30 min. A yellow translucent solution was obtained in all cases and stored at room temperature and protected from light.

Replacement of capping agent with CLK-W peptides: Aliquots of the WP1, WP2, or WP3 peptides were added to fresh citrate@AgNP solutions of known volume and concentration. Tested peptide concentrations were 0.1, 0.5, 1, 5, 10, 20, 50 and 100 μM . Unless otherwise indicated, all the experiments were done in triplicate.

Peptide capped nanosilver stability assessments: The colloidal stability of WPeptide@AgNPs was assessed through surface plasmon band (SPB) stability, thermostability, and ionic stress. For SPB stability, AgNPs were incubated with one of the three peptides at 0.1, 0.5, 1, 5, 10 or 20 μM and the absorbance spectra was measured in a Libra S50 UV-Vis spectrophotometer (Biochrom, Cambridge, UK) at various incubation times (5 min, 15 min, 30 min, 45 min, 2 h, 6 h, 24 h and 4 days) at room temperature. Maximum absorbance and width was plotted over time and the optimum incubation time was

determined to be between 15-30 min, thus, for the experiments that follow, peptides were incubated for the aforementioned amount of time with the nanoparticles before testing began.

For thermostability, two experiments were done, one at 37°C and the other at 98°C. At 37°C, WPeptide@AgNPs (5, 10 and 20 µM) in 1mL aliquots and incubated in a Model 400 Hybridization Incubator (Robbins Scientific, San Diego, USA) for 0 min, 45 min, 6 h, 24 h and 48 h and the SPB measured by using the spectrophotometer. For the second thermostability experiment, WPeptide@AgNPs at 10 µM were heated at 98°C and the SPB measured at 0, 15, 45 and 120 min.

For ionic stress stability. WPeptide@AgNPs (at 10 µM peptide concentration) were mixed with a 10 mM NaCl solution and the SPB was measured as control, right after mixing, at 6 h, 24 h and 48 h using a Synergy Mx multi-mode microplate reader (BioTEK, Winooski, USA)

SPB kinetics: The kinetics of the oxidation reaction was assessed by following the SPB of the NPs. WPeptide@AgNPs at 5, 10 and 20 µM as well as Citrate@AgNPs were incubated with 10 mM AAPH at 37°C and further, the SPB was measured at 0, 10, 30, 60, 120 and 300 s.

Tryptophan fluorescence measurements: Peptides tryptophan fluorescence was followed by using a Perkin-Elmer LS-50B Fluorescence Spectrophotometer (Waltham, USA). Firstly, the fluorescence of each peptide was evaluated at different concentrations (1, 5 and 10 µM). Spectrophotometer settings as follow: 10 nm slits, 295 nm excitation wavelength, and emission wavelength of 305-500 nm scanning window. Then, 10 mM of AAPH was added and the fluorescence was measured at 0, 10, 30, 60 and 120 min. Quenching rates were calculated. Secondly, under same settings conditions the fluorescence of each WPeptide@AgNPs (same peptides concentrations) was measured. Thirdly, the fluorescence of 10 µM free tryptophan and Tryptophan@AgNPs was measured without and with AAPH (same concentration and time points) to then compared it to the WPeptides. Inner filter corrections were also made during this experiment. Nanosecond fluorescence lifetime for the peptides were measured in an EasyLife system using a 290 nm pulse LED and an emission band pass filter centered at 350 nm.

Peroxide assays: Peroxide production was assessed by using a Thermo Scientific Pierce Quantitative Peroxyde Assay Kit (Thermo Scientific, Massachusetts, USA). Briefly, the samples tested were free WPeptides (10 μ M) and WPeptide@AgNPs (10 μ M). Each sample was incubated by 5 min or 2h with AAPH at 37°C and then was quickly quenched using ice. The kit's protocol was then followed, and further, peroxide concentrations of each sample was calculated by measuring the absorbance 595 nm and using a H₂O₂ standard curve.

Synthesis of Small Silver Clusters: 175 μ L of cold aqueous 0.01 g/mL (10 μ mol) AgNO₃ (99.0%, Sigma Aldrich) was added to 13.3 μ mol of peptide (abm Inc.) dissolved in 800 μ L Milli-Q water in a 20 mL vial. The mixture was stirred for five minutes in an ice-water bath. 20 equivalents (200 μ mol) of NaBH₄ (98%, Sigma Aldrich) reducing agent was added to the mixture, and the cap was left off to prevent gaseous build up. The reaction mixture was left to stir for 30 minutes. It turned a dark brown colour (eq. 1). The solution was washed with acetonitrile, at 3 times the volume of the mixture. The nanoclusters were precipitated via centrifugation at 6000 rpm. The samples were dried with nitrogen, sealed tightly, and stored in the fridge.



Characterization of Small Silver Clusters: Absorbance measurements were acquired for samples in a 2 mm quartz cuvette by a Varian Cary 60 UV-Vis Spectrophotometer. Samples were absorbance matched at 490 nm for fsTAS measurements. Absorbance spectra were collected (as seen below) for P3 and WP3 clusters, and for P2 and WP2 clusters.

fsTAS for Small Silver Clusters: Transient absorbance measurements were acquired for samples in a 2 mm quartz cuvette by an Ultrafast HELIOS Fire Femtosecond Transient Absorption Spectrometer. The samples were excited with a pump of 340 nm with 250 fs pulses and a repetition rate of 500 Hz (< 1 mJ/pulse). Surface Xplorer software was used to analyze the transient absorption spectra, kinetics, and to perform corrections for chirp signals and spectral noise. 2D transient fsTAS plots are shown in Fig. S5-S8, for each of the samples of Ag clusters, with and without tryptophan labeled peptides as stabilizing ligands.

Atomistic Modeling: The peptide models were generated using the Chimera software.² The Ag{111} surface was constructed according to the model of Hughes et al.³ This procedure was described in detail in previous work of our group.^{4, 5} All the systems were assembled using VMD 1.9.3 software.⁶

Molecular Dynamics Methods: All classical molecular dynamics simulations were executed using the NAMD 2.12 software⁷ in an explicit solvent environment, employing the TIP3P water model used by the CHARMM force field.^{8, 9} The area for each system was fixed in the xy-plane and the Langevin piston method¹⁰ was allowed to fluctuate only along the z-axis. The temperature and pressure were maintained stable at 300 K and 101.325 kPa (1.0 atm). Periodic boundary conditions were employed using the particle-mesh Ewald electrostatics algorithm¹¹ and smooth switching of van de Walls forces between 0.8-0.9 nm cut-off, after which isotropic long-range approximation was employed. The mass of peptide-H atoms was multiplied by a factor of 3 (to 3.0240 Da), mass that was subtracted from the heavy atoms to which these H atoms were attached,¹² this mass repartition allows us to integrate the equation of motion with a time step of 4 fs.^{13, 14} The mass distribution of water molecules was not altered, but the length of its covalent bonds involving hydrogen atoms were constrained using the RATTLE and SETTLE algorithms.¹⁵ For each peptide (WP1, WP2 and WP3) system, we performed 20,000 steps of energy minimization followed by 10 ns of equilibration before beginning the free energy calculations. VMD 1.9.4 was used for visualizations, analysis and molecular renderings.

Free Energy Calculations: Applying the adaptive biasing force (ABF) method¹⁶⁻¹⁸ implemented through the Colvars module¹⁹ in NAMD,⁷ was possible to calculate the potential of mean force (PMF) of the peptides adsorption to the AgNPs surface. We sampled two transition coordinates to identify the conformational free energy minima: Z , as the z-distance from the center of mass of the peptide to the AgNP surface, and orientation (ζ) of the peptide relative to the surface, both transition coordinates were described by our group previously.^{4, 5} The first collective variable, Z , was sampled using multiple windows (three windows, 4-16, 14-24 and 22-32 Å for all peptides), and the second collective variable was sampled using a

single window $-40 \leq \zeta \leq 40$ Å for a total time of 6.41 ms, 10.65 ms, and 7.76 ms for WP1, WP2 and WP3 respectively.

Packed Models: Full-loaded peptide surfaces were built using a set of 10 conformations representative of the free-energy minima calculated previously for P1W, P2W and P3W (see Fig 3A). The free-energy calculations were performed on a single tagged peptide located at 25Å from the surface on which were sampled the Z and ζ transition coordinates like was described above. An additional harmonic restraint to avoid to the packed peptides to leave more than 20Å from the surface was implemented through the Colvars module.¹⁹ The Z collective variable was sampled in a multiple window scheme such as was described previously, and ζ was also sampled using multiple windows ($-40 \leq \zeta \leq -8$, $-10 \leq \zeta \leq 10$ and $-8 \leq \zeta \leq 40$) reaching a total of 9 windows per system for a total time of 9.51 ms, 19.47 ms, 11.14ms for WP1, WP2 and WP3 respectively.

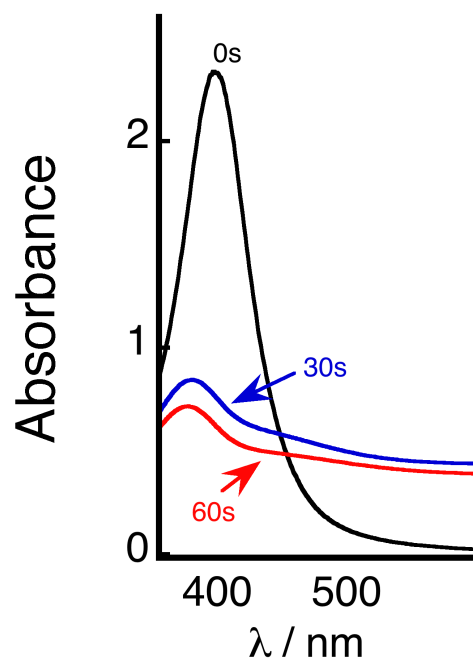


Figure S1. Plasmonic absorption for citrate capped nanosilver in the presence of 10 mM AAPH at 37°C, measured 30 and 60 seconds after addition of the peroxy radical generator.

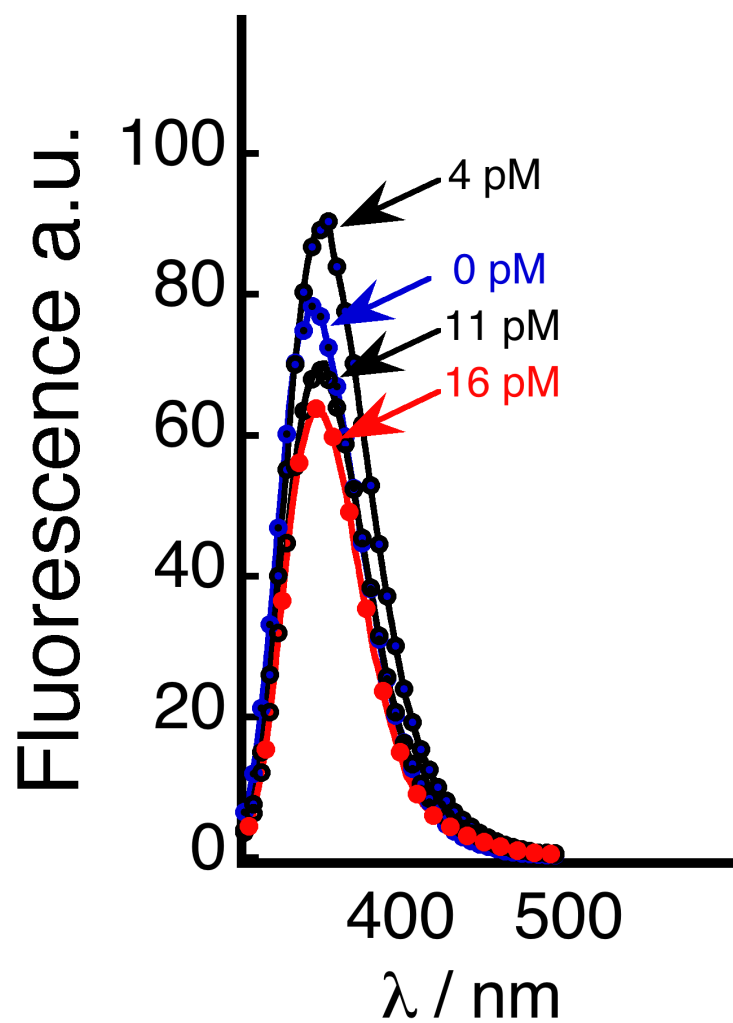


Figure S2. Effect of nanosilver addition on the fluorescence emission of WP1. Nanosilver concentration added to WP1 solution is showed in the figure in picomolar concentration. Excitation wavelength was 295 nm. All measurements were carried out at room temperature.

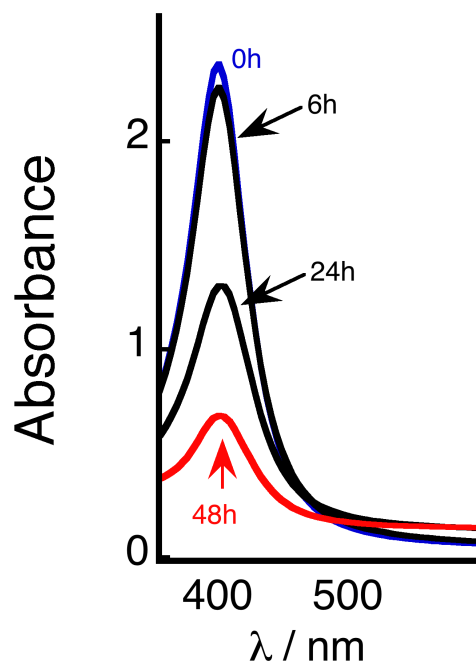


Figure S3. Effect of 10 mM NaCl media in the surface plasmon band absorption for nanosilver without peptides. Spectra were measured at different time points post the incubation started at 37°C.

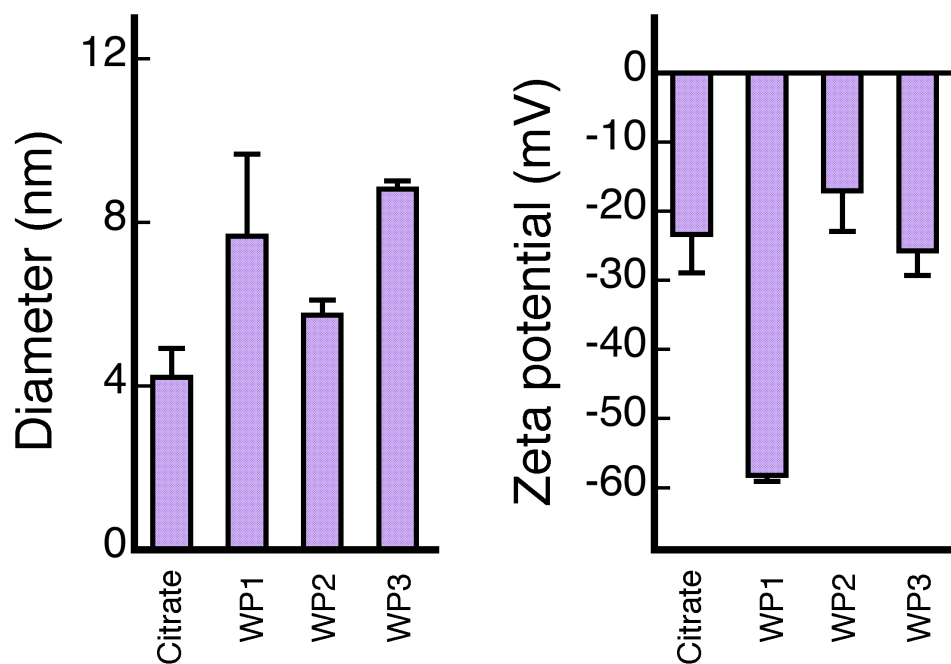


Figure S4. Hydrodynamic size (left) and surface charge (right) for nanosilver without (citrate capped) and with 10 μM of WP1, WP2, and WP3. Experiments were carried out at room temperature (n=3).

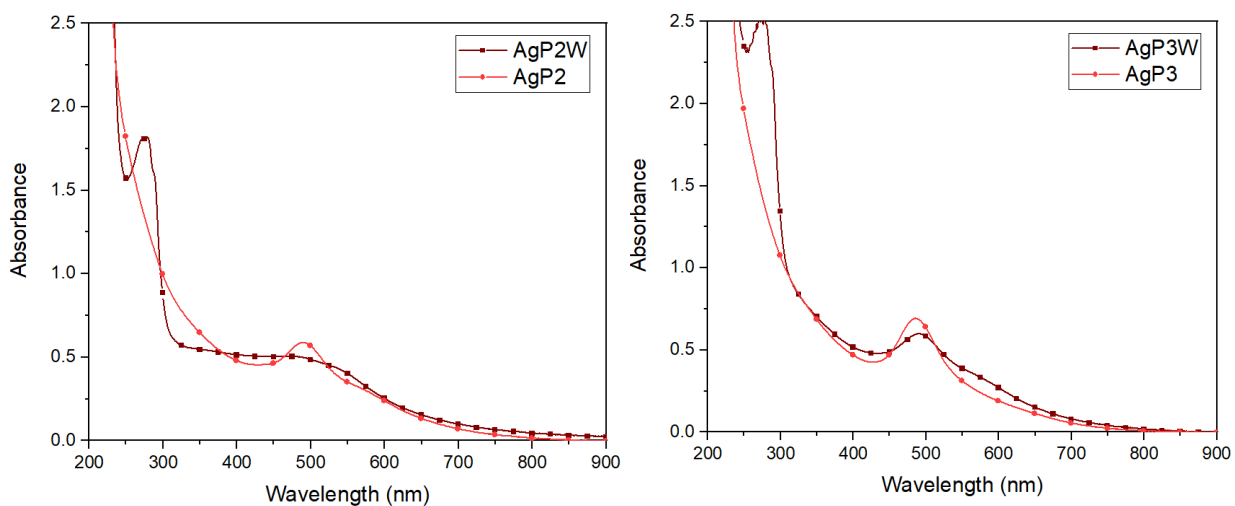


Figure S5. Steady state absorbance spectra of Ag cluster samples stabilized by peptides WP2 (left) and WP3 (right) both with and without tryptophan as indicated.

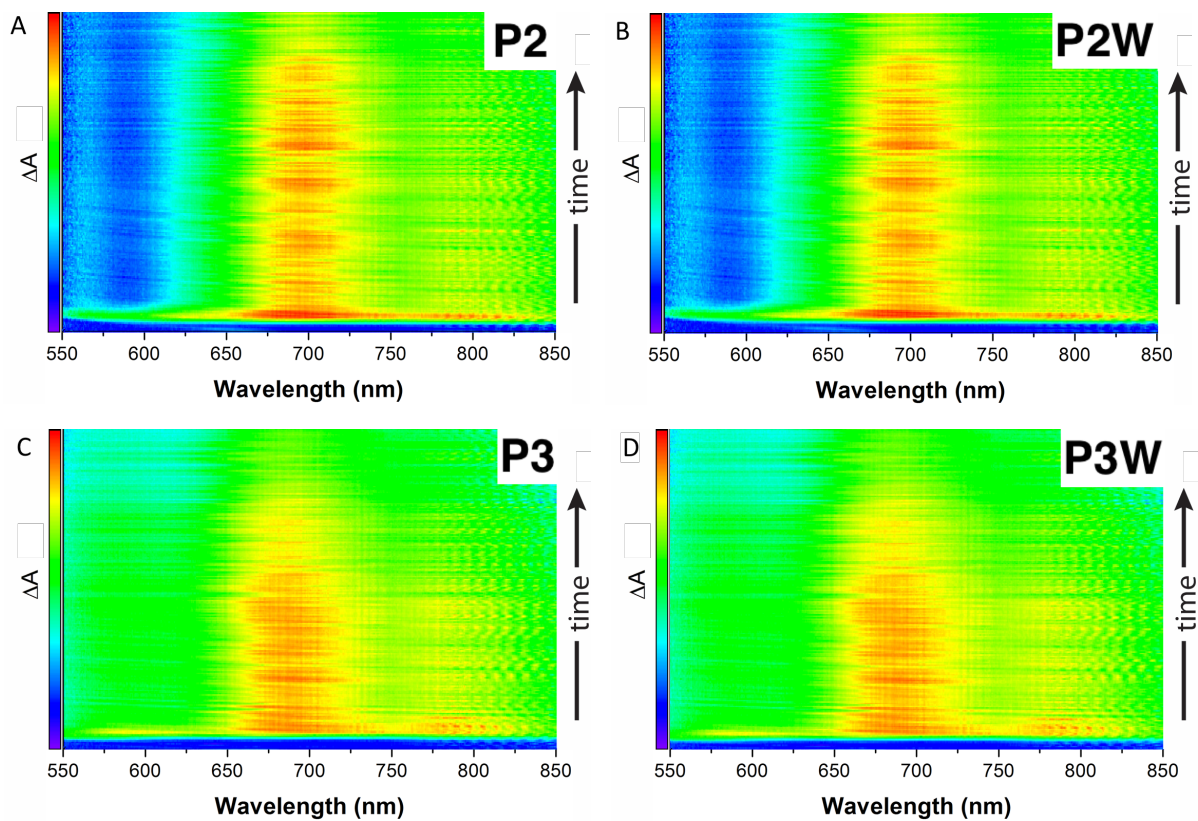


Figure S6. 2D fsTAS profiles for Ag clusters stabilized by P2, WP3, P3 and WP3 as indicated in the inset. The coloured scale bar indicates the magnitude of ΔA for the excited state and the vertical axis in each case is time ranging from ~ 1 ps before laser excitation to a delay of 6 ns after excitation (note that this is not a linear scale).

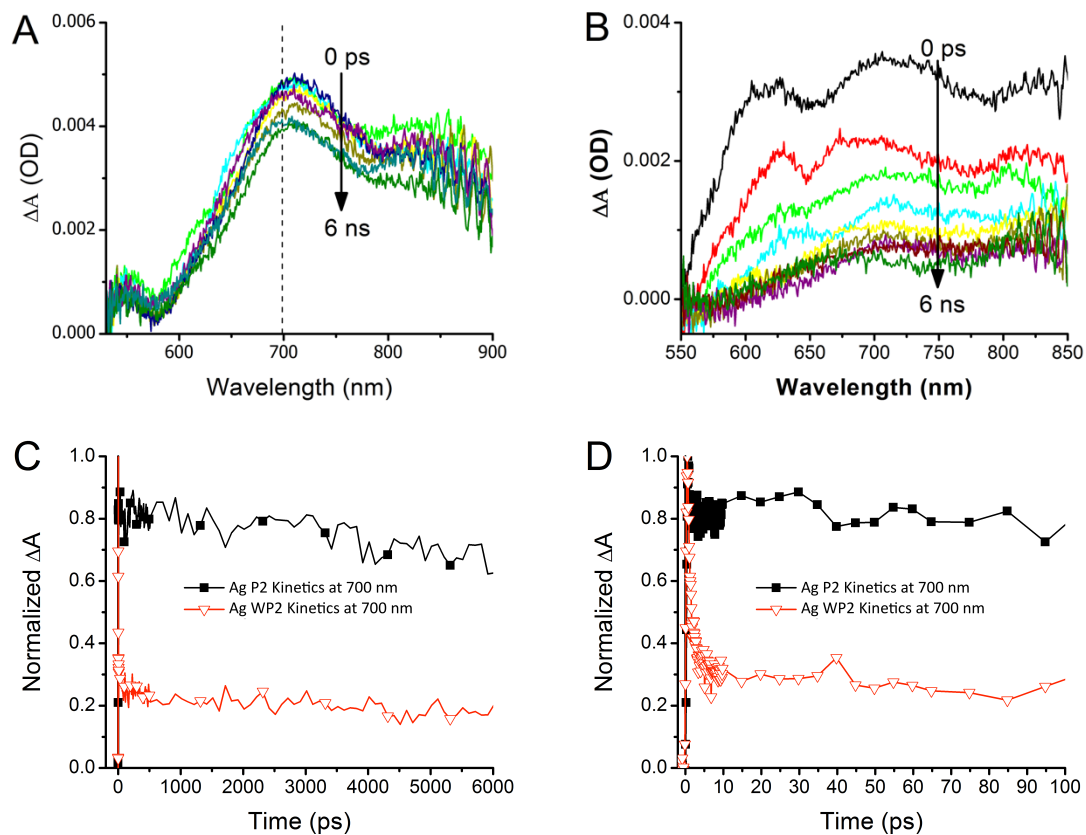


Figure S7. Transient absorption spectra for Ag clusters stabilized with P2 (a), WP2 (b), and the kinetic profiles of the excited state relaxation for each as indicated (c) and (d). Panel (d) is included to highlight the rapid relaxation component that is very prominent for P2 with tryptophan, and which indicates the electronic interaction between tryptophan and the excited silver.

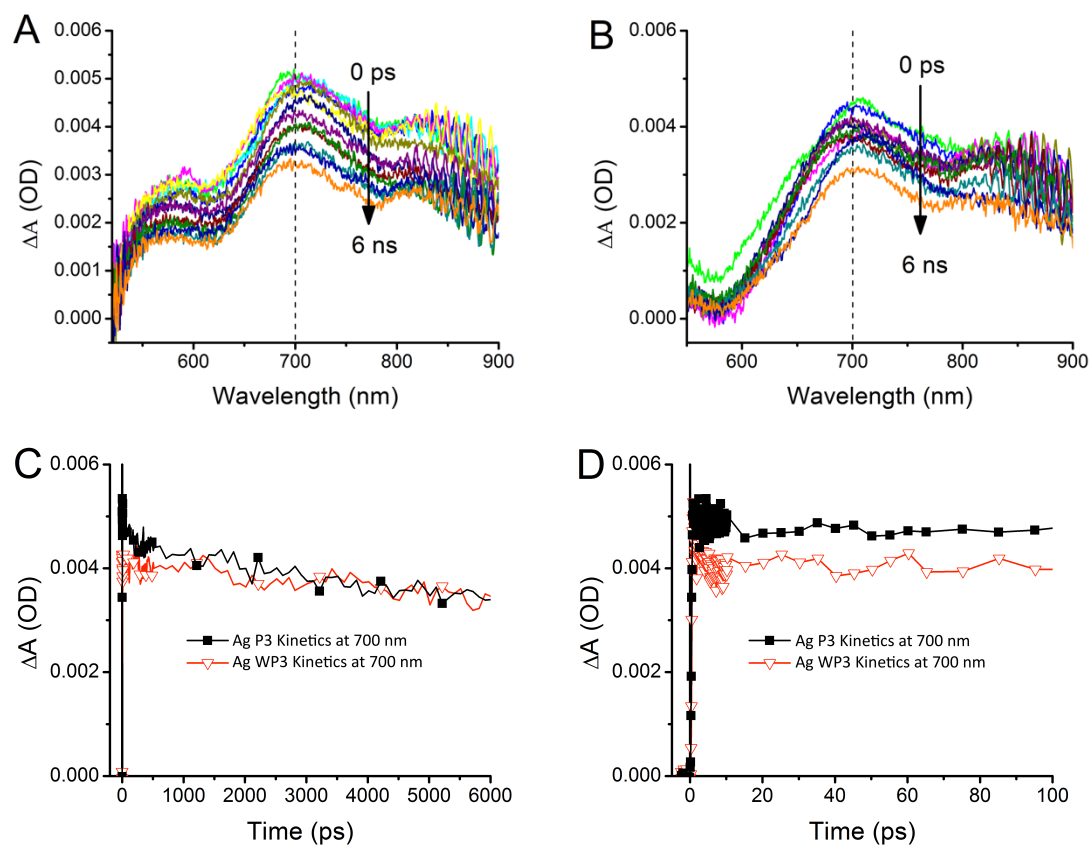


Figure S8. Transient absorption spectra for Ag clusters stabilized with P3 (a), WP3 (b), and the kinetic profiles of the excited state relaxation for each as indicated (c) and (d). Panel (d) is included to highlight the rapid relaxation component that is very prominent for P2 with tryptophan, and which indicates the electronic interaction between tryptophan and the excited silver; note that the interaction is less important (less quenching of the excited state) for P3 than P2.

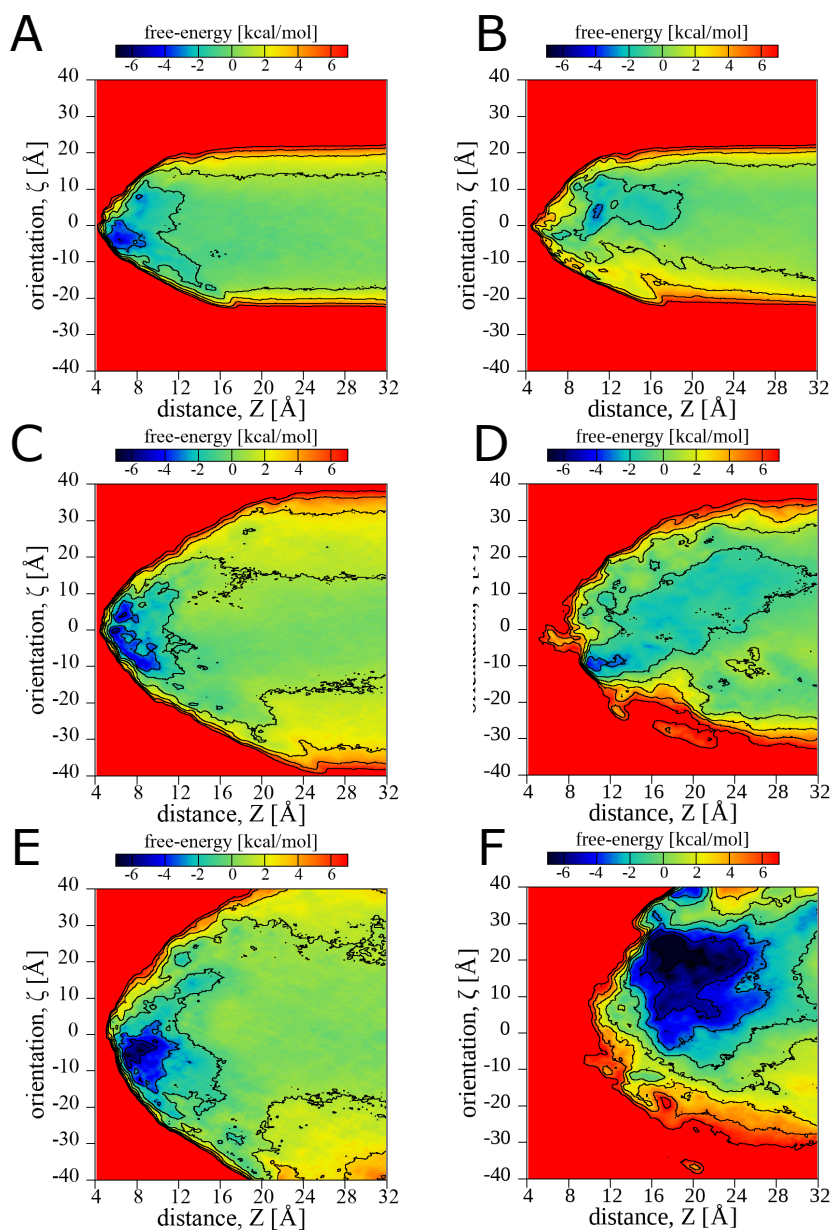


Figure S9. Characterization of the binding mode of CLK-GP-Hyp-W (WP1), CLK-(GP-Hyp)3-W (WP2), and CLK-(GP-Hyp)5-W (WP3) to the AgNP surface through molecular simulations. (Left) Two-dimensional free energy landscapes of the single peptides (A) WP1, (C) WP2 and (E) WP3 to an AgNP surface. The free energy was anchored to the average PMF at large distances of the peptide to the surface ($Z > 29$ Å). (Right) Two-dimensional free energy landscapes for peptides (B) WP1, (D) WP2 and (F) WP3 to an AgNP surface capped with 10 peptides.

References

1. K. G. Stamplecoskie and J. C. Scaiano, *J. Am. Chem. Soc.*, 2010, **132**, 1825-1827.
2. E. F. Pettersen, T. D. Goddard, C. C. Huang, G. S. Couch, D. M. Greenblatt, E. C. Meng and T. E. Ferrin, *J. Comp. Chem.*, 2004, **25**, 1605-1612.
3. Z. E. Hughes, L. B. Wright and T. R. Walsh, *Langmuir*, 2013, **29**, 13217-13229.
4. M. Ahumada, E. Jaques, C. Andronic, J. Comer, H. Poblete and E. Alarcon, *J. Mat. Chem. B*, 2017, **5**, 8925-8928
5. H. Poblete, A. Agarwal, S. S. Thomas, C. Bohne, R. Ravichandran, J. Phospase, J. Comer and E. I. Alarcon, *Langmuir*, 2016, **32**, 265-273.
6. W. Humphrey, A. Dalke and K. Schulten, *J. Mol. Graph.*, 1996, **14**, 33-38.
7. J. C. Phillips, R. Braun, W. Wang, J. Gumbart, E. Tajkhorshid, E. Villa, C. Chipot, R. D. Skeel, L. Kalé and K. Schulten, *J. Comp. Chem.*, 2005, **26**, 1781-1802.
8. A. D. MacKerell, D. Bashford, M. Bellott, R. L. Dunbrack, J. D. Evanseck, M. J. Field, S. Fischer, J. Gao, H. Guo, S. Ha, D. Joseph-McCarthy, L. Kuchnir, K. Kuczera, F. T. K. Lau, C. Mattos, S. Michnick, T. Ngo, D. T. Nguyen, B. Prodhom, W. E. Reiher, B. Roux, M. Schlenkrich, J. C. Smith, R. Stote, J. Straub, M. Watanabe, J. Wiórkiewicz-Kuczera, D. Yin and M. Karplus, *J. Phys. Chem. B*, 1998, **102**, 3586-3616.
9. R. B. Best, X. Zhu, J. Shim, P. E. M. Lopes, J. Mittal, M. Feig and A. D. MacKerell, *J. Chem. Theory Comput.*, 2012, **8**, 3257-3273.
10. S. E. Feller, Y. Zhang, R. W. Pastor and B. R. Brooks, *J. Chem. Phys.*, 1995, **103**, 4613-4621.
11. T. Darden, D. York and L. Pedersen, *J. Chem. Phys.*, 1993, **98**, 10089-10092.
12. C. W. Hopkins, S. Le Grand, R. C. Walker and A. E. Roitberg, *J. Chem. Theory Comput.*, 2015, **11**, 1864-1874.
13. H. Poblete, I. Miranda-Carvajal and J. Comer, *J. Phys. Chem. B*, 2017, **121**, 3895-3907.
14. E. I. Alarcon, H. Poblete, H. Roh, J.-F. Couture, J. Comer and I. E. Kochevar, *ACS Omega*, 2017, **2**, 6646-6657.
15. M. Shuichi and K. P. A., *J. Comp. Chem.*, 1992, **13**, 952-962.
16. E. Darve and A. Pohorille, *J. Chem. Phys.*, 2001, **115**, 9169-9183.
17. J. Hénin and C. Chipot, *J. Chem. Phys.*, 2004, **121**, 2904-2914.
18. J. Comer, J. C. Gumbart, J. Hénin, T. Lelièvre, A. Pohorille and C. Chipot, *J. Phys. Chem. B*, 2015, **119**, 1129-1151.
19. G. Fiorin, M. L. Klein and J. Hénin, *Mol. Phys.*, 2013, **111**, 3345-3362.